EasyChair Preprint

№ 387

# Design of Lattice Structures with Graded Density Fabricated by Additive Manufacturing

Wenjin Tao, Yong Liu, Austin Sutton, Krishna Kolan and Ming C. Leu



August 1, 2018

# DESIGN OF LATTICE STRUCTURES WITH GRADED DENSITY FABRICATED BY ADDITIVE MANUFACTURING

**Wenjin Tao**
Department of Mechanical and Aerospace Engineering,
Missouri University of Science and Technology
Rolla, MO 65409, USA
wt6c2@mst.edu

**Yong Liu**
School of Mechanical and Precision Instrument Engineering,
Xi'an University of Technology
Xi'an, 710048, China
liuyong@xaut.edu.cn

**Austin Sutton**
Department of Mechanical and Aerospace Engineering,
Missouri University of Science and Technology
Rolla, MO 65409, USA
atsfk6@mst.edu

**Krishna Kolan**
Department of Mechanical and Aerospace Engineering,
Missouri University of Science and Technology
Rolla, MO 65409, USA
kolank@mst.edu

**Ming C. Leu**
Department of Mechanical and Aerospace Engineering,
Missouri University of Science and Technology
Rolla, MO 65409, USA
mleu@mst.edu

## ABSTRACT

Lattice structures fabricated by Additive Manufacturing (AM) processes are promising for many applications, such as lightweight structures and energy absorbers. However, predicting and controlling of their mechanical behaviors is challenging due to the complexity of modeling and the uncertainties exist in the manufacturing process. In this paper, we explore the possibilities enabled by controlling the local densities. A set of lattice structures with different density gradients are designed using an implicit isosurface equation, and they are manufactured by Selective Laser Melting (SLM) process with 304L stainless steel. Finite element analysis and compression test are used to evaluate their mechanical properties. The results demonstrate the strong correlations between the structural gradient and the mechanical behavior. Introducing the density gradient provides more possibilities in the design phase, which can be used to further customize the design both structurally and functionally.

## INTRODUCTION

The fast-growing Additive Manufacturing (AM) technologies have been deployed in a wide range of industries, such as aerospace, automotive, biomedical, and energy [1]. Profiting from the 'layer-by-layer' building manner of the AM processes, parts from various materials with unprecedent complexities can be fabricated in one build, e.g., lattice structures.

The superior properties AM lattice structure possesses make it a promising solution for many applications, such as lightweight structures, heat exchangers, energy absorbers, biomedical scaffold, and catalyst carrier [2-4]. Current studies and applications are more focused on the lattice structure with uniform density [5-7] than that with graded density, because its CAD model is easier to design and properties are easier to analyze. However, lattice structures with graded density are able to provide more design possibilities, which can be used to further customize their mechanical properties.

In this paper, we explore the possibilities enabled by controlling the local densities of lattice structures. A set of lattice structures with different density gradients were designed using an implicit Triply Periodic Minimal Surfaces (TPMS). One of the advantages of using this design method is that the graded density can be easily introduced by adding controlling terms into the surface equation. A genetic algorithm was used to find the best design parameters. Then these lattice structures were manufactured by Selective Laser Melting (SLM) process with the material of 304L stainless steel. Finite element analysis and compression test were employed to evaluate their mechanical properties and failure behavior.

## MATERIAL AND METHODS

### Design of lattice structure with graded density

Different methods for designing lattice structures have been discussed in [2]. Due to the flexibility in density control, we chose the implicit surface based method in the structure designing. This method uses implicit equation(s) to represent the surface of a lattice structure in three-dimensional space. For example, Eq. (1) defines a set of points $(x, y, z)$ that make $F = 0$. All these points could form the surface of a lattice structure.

$$F(x, y, z) = 0 \quad (1)$$

$$F(x, y, z) = cos(2\pi x) + cos(2\pi y) + cos(2\pi z) - a\big(cos(\pi x)cos(\pi y) + cos(\pi y)cos(\pi z) + cos(\pi z)cos(\pi x)\big) + b + c\pi z \quad (2)$$

To have a truss-like architecture that is manufacturable for SLM process without building any support structures, Eq. (2) was used in this research, where $a, b\ and\ c$ are parameters controlling the architecture to be tuned. A MATLAB routine was developed for implementing Eq. (2) to generate the lattice structure and then export an STL file.

The volume of a polyhedron with $n$ planar polygonal faces $F_i, i \in [1, n]$ can be calculated by Eq. (3) [8]:

$$V_{Polyhedron} = \frac{1}{3}\left|\sum_{i=1}^{n}(Q_i \cdot N_i)\, Area(F_i)\right| \quad (3)$$

where $Q_i$ is an arbitrary point on $F_i$, and $N_i$ is the unit normal vector of $F_i$. An STL model can be taken as a polyhedron whose polygonal faces are all triangles, thus, the volume of an STL model can be derived from Eq. (3) as:

$$V_{stl} = \frac{1}{6}\sum_{i}^{n} v_1^i\left[(v_2^i - v_1^i) \times (v_3^i - v_1^i)\right] \quad (4)$$

To define the values for $a, b\ and\ c$ in Eq. (2), a set of baseline parameters were chosen, $a = 1, b = c = 0$. The density gradient was adjusted by the value of $c$. To keep a constant volume fraction while changing the density gradient for comparison purpose, a genetic algorithm was used to search the value of $b$, given $a\ and\ c$, and the target of volume fraction.

Five designs of lattice structure with different density gradients are illustrated in Fig. 1. Their design parameters are listed in Table 1. All the designs have the same volume fractions, which is 56.61%.

Table 1. Design parameters of the 5 lattice structures with different density gradients.

| No. | a | b | c | $V_{stl}(mm^3)$ |
|---|---|---|---|---|
| 0 | 1.0 | 0.00000 | 0.000 | 978.2444 |
| 1 | 1.0 | -0.19115 | 0.010 | 978.2433 |
| 2 | 1.0 | -0.38895 | 0.020 | 978.2440 |
| 3 | 1.0 | -0.59331 | 0.030 | 978.2427 |
| 4 | 1.0 | -0.80522 | 0.040 | 978.2425 |
| 5 | 1.0 | -1.02126 | 0.050 | 978.2470 |

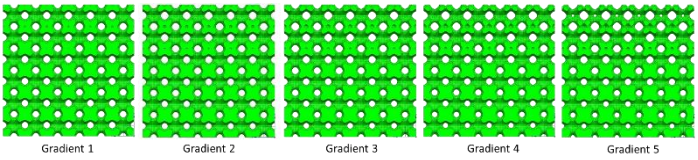


**Figure 1: The designed lattice structures with different density gradients.**

### Selective Laser Melting (SLM) process

Selective laser melting (SLM) utilizes a laser to melt and consolidate particles for creation of three-dimensional components directly from their digital models. In this study, the SLM process was exploited for its manufacturability of intricate features to build several lattice structures. All parts were fabricated by a Renishaw AM250 SLM system with 304L stainless steel powder as the raw material. The AM250 is equipped with a 200W Nd-YAG 1070 nm Gaussian pulsed laser with a beam spot size of approximately 70 μm at the powder-bed. Before manufacturing, the build chamber was inerted through a purging process with argon to reduce the oxygen content to a stabilized value below 1000 ppm to minimize part oxidation. During operation, a constant 400 $ft^3$/min of argon crossflow was induced to maintain an inert atmosphere as well as for the removal of melt pool ejecta from the laser beam path. Once built, the parts were removed from the substrate using a Sodick VZ500LH wire EDM machine to reduce the likelihood of damage induced on the parts.

### Powder characterization

The powder used for fabrication of the lattice structures was argon gas-atomized 304L stainless steel powder produced by LPW Technology. An image of the powder was acquired using a scanning electron microscope (SEM), which can be seen in Fig. 2(a). The particle size distribution was collected using an ASPEX SEM with its Automated Feature Analysis (AFA) capability for measurement of the projected area and perimeter of at least 2500 particles. Conversion of the number distribution to a volume distribution assuming perfect spheres for each particle was performed, for which the resulting distribution can be seen in Fig. 2(b). Here, the D10, D50, and D90 of the as-received 304L powder was calculated to be 19.2 μm, 27.5 μm, and 38.3 μm, respectively. The composition of the powder provided by the supplier is shown in Table 2.

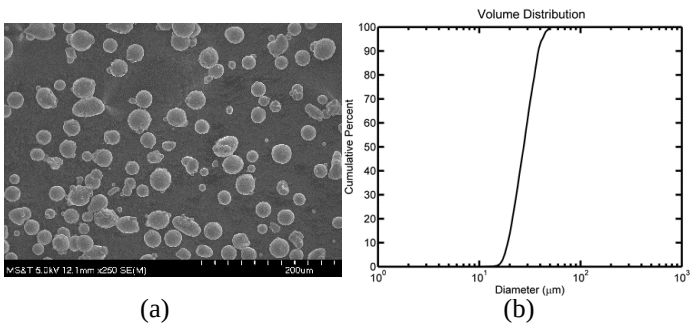


(a) (b)

**Figure 2: (a) An SEM image of 304L particles; (b) the corresponding volumetric distribution of the powder.**

Table 2. 304L chemical composition provided by LPW Technology.

| | C | Cr | Cu | Fe | Mn | N | Ni | O | P | S | Si |
|---|---|---|---|---|---|---|---|---|---|---|---|
| Wt % | 0.018 | 18.4 | < 0.1 | Bal | 1.4 | 0.06 | 9.8 | 0.02 | 0.012 | 0.005 | 0.63 |

### Finite element analysis

A three-dimensional linear finite element model was created, and compression simulations were implemented using ABAQUS to investigate the elastic properties of the designed lattice structures. The isotropic characteristics of 304L stainless steel were assigned to the model with Young's modulus of 193 GPa and Posson's ratio of 0.27. The boundary conditions for each lattice structure are shown in Fig. 3(a). During the compression simulations, the bottom nodes were constrained in the $XY$ plane, and force of 5,000 N was loaded on top of the lattice structure along the $Z$ direction. The model was meshed using tetrahedron element with the size of 0.2 mm, which is shown in Fig. 3(b).

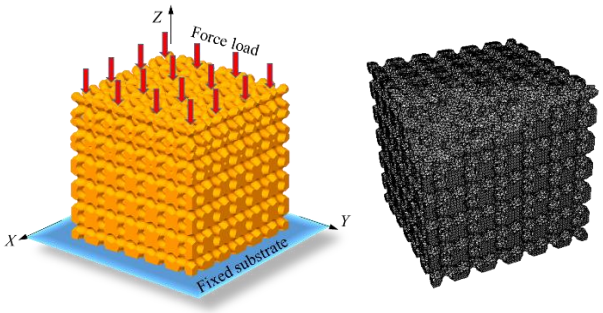


(a) (b)

**Figure 3: (a) Boundary conditions and (b) meshed model of a lattice structure.**

### Experimental evaluation

To experimentally evaluate the mechanical behavior, compression tests were conducted on the fabricated specimens. The compression tests were performed at room temperature on an MTS material testing system with a 100 kN load cell (Fig. 4). These specimens were compressed in parallel to the building direction between two hardened loading heads at a rate of 0.5 mm/min. The test stopped when the load reached 70% of its maximum limit. The force measured from the load sensor and the displacement of the moving head were recorded using a computer.

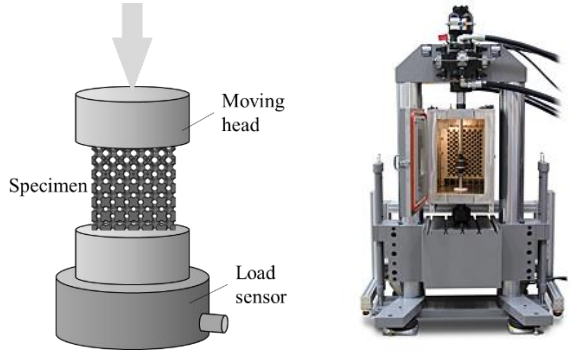


**Figure 4: (a) Schematic diagram of the compression test and (b) photo of the testing machine.**

## RESULTS AND DISCUSSION

The designed lattice parts were manufactured and removed from the substrate as discussed in the previous section. Figure 5 presents the 5 printed lattice structures with different density gradients. No support structures were needed during the building process because they are self-supported.

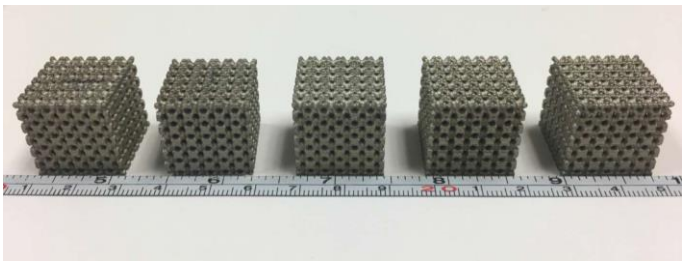

**Figure 5: Lattice structures designed with different density distributions.**

Figure 6 shows the stress distributions from the FEA simulations at different cases, where the colors represent the magnitude of the stress. The stress of the baseline model ('gradient 0') is nearly evenly distributed. While for the others, the elements at the upper sparse region have larger stress than the lower dense region. With increasing the gradient, the stress at the upper layers becomes larger while that at the lower layers becomes smaller. This is because that the gradient makes the sparse part weaker while the dense part stronger.

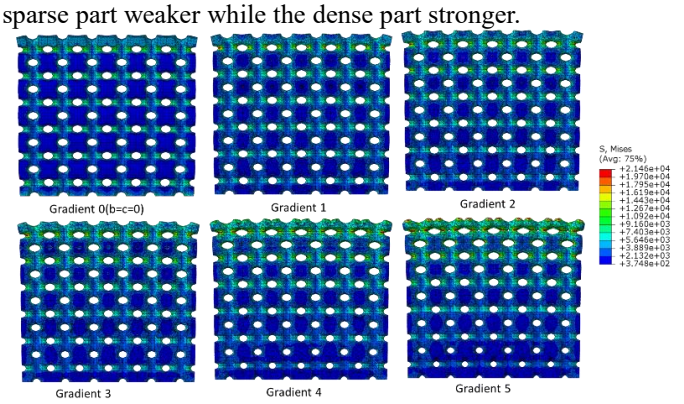


**Figure 6: Stress distribution of each lattice structure.**

To investigate the nodal displacements along the $Z$ direction at different locations, 13 observation points on a lattice structure were selected (Fig. 7(a)). Their displacements were measured for each of the 6 cases, which are plotted in Fig. 7(b). A quadratic regression was employed to fit the relation between the displacement and the $Z$ location. The nodal displacement of the lattice structure without density gradient ('gradient 0') increases approximately linearly with the increase of the Z value. While for a lattice structure with density gradient, the displacement climbs quadratically as its Z value increases.

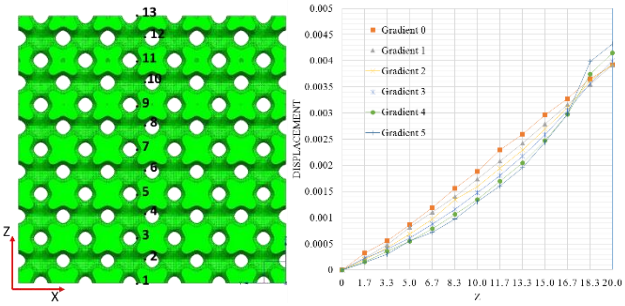


(a) (b)

**Figure 7: Displacement at different locations along the Z direction.**

Two specimens, 'gradient 3' and 'gradient 5' shown in Fig. 6, were tested. To have a better observation of the compressive behavior, each specimen was cut into 4 samples with the dimensions of $10\,mm \times 10\,mm \times 20\,mm$. Two samples from each lattice structure were used in the compression test. The results for the 4 samples are plotted in Fig. 8. Samples of 'gradient 3' have relatively larger slopes in the elastic deformation region on the load-displacement curves, compared to the samples of 'gradient 5'. After that, the load increases slowly with increase in displacement because of the plastic deformation of the sparse region in the lattice structure. Then the load climbs again with increase in displacement because the pores are vanished and the lattice structure starts being densified.

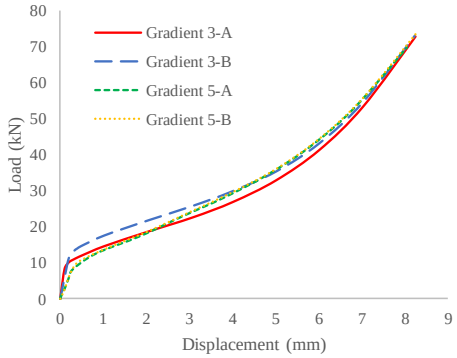


**Figure 8: Result of the compression test.**

Each of the 4 samples was loaded until reaching the preset load limit. It was observed that as the loading head moved down, struts near the top began to bend and caused plastic deformation (Fig. 9(a)). All the samples deformed layer-by-layer from the top to bottom. Figure 9(b) shows the comparison between the samples of 'gradient 3' before and after the compression test.

## CONCLUSION

In this paper, we have investigated the mechanical characteristics and failure behavior of lattice structures with graded density manufactured by Selective Laser Melting (SLM) process with the material of 304L stainless steel. The results of this study are summarized below:

- By using an implicit surface based method and a genetic algorithm, a lattice structure with graded density can be designed accurately for a volume fraction target.
- Finite element analysis shows that the stress and deformation distributions of a graded lattice structure are correlated with the density gradient. The region with larger porosity has larger stress and deformation.
- The experimental results show that the lattice structure with graded density fails by plastic yield gradually from the upper sparse region to the bottom dense region, which agrees with the FEA results and demonstrates the correlation between the gradient and the failure behavior.
- Overall, this study points out that adjusting the density distribution to improve the mechanical behavior would be of value in the design phase to design a lattice structure both geometrically and functionally.

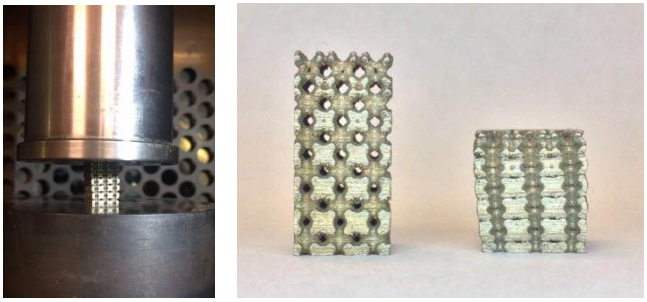

(a) (b)

**Figure 9: Failure behavior (a) in the compression process; (b) samples before and after the compression test.**

## ACKNOWLEDGMENT

This study was supported by National Natural Science Foundation of China (61402361) and the Intelligent Systems Center at the Missouri University of Science and Technology.

## REFERENCES

[1]. Guo, Nannan, and Ming C. Leu. "Additive manufacturing: technology, applications and research needs." Frontiers of Mechanical Engineering 8.3 (2013): 215-243.

[2]. Tao, Wenjin, and Ming C. Leu. "Design of lattice structure for additive manufacturing." Flexible Automation (ISFA), International Symposium on. IEEE, 2016.

[3]. Li, Xin, et al. "Catalytic cracking of n-hexane for producing light olefins on 3D-printed monoliths of MFI and FAU zeolites." Chemical Engineering Journal (2017).

[4]. Murphy, C., et al. "3D bioprinting of stem cells and polymer/bioactive glass composite scaffolds for bone tissue engineering." International Journal of Bioprinting 3.1 (2017): 1-11.

[5]. Xiao, Lijun, et al. "Mechanical properties of open-cell rhombic dodecahedron titanium alloy lattice structure manufactured using electron beam melting under dynamic loading." International Journal of Impact Engineering 100 (2017): 75-89.

[6]. Geng, Xiaoliang, et al. "A FEM study on mechanical behavior of cellular lattice materials based on combined elements." Materials Science and Engineering: A (2017).

[7]. Montazerian, H., et al. "Porous scaffold internal architecture design based on minimal surfaces: A compromise between permeability and elastic properties." Materials & Design 126 (2017): 98-114.

[8]. Arvo, J. ed., 2013. Graphics gems II. Elsevier.